Article:
Mishra, S., Hunter, T.N., Pant, K.K. et al. (2024) Green Deep Eutectic Solvents (DESs) for Sustainable Metal Recovery from Thermally Treated PCBs: A Greener Alternative to Conventional Methods. ChemSusChem, 17 (8). e202301418. ISSN: 1864-5631

https://doi.org/10.1002/cssc.202301418

Green Deep Eutectic Solvents (DESs) for Sustainable Metal Recovery from Thermally Treated PCBs: A Greener Alternative to Conventional Methods

Snigdha Mishra [1][2], T.N. Hunter [2], K.K. Pant* [1][3], David Harbottle* [2]

[1] Green and Sustainable Engineering Lab, Department of Chemical Engineering, IIT Delhi, Hauz Khaz, Delhi, 110016, India
[2] School of Chemical and Process Engineering, University of Leeds, Leeds, LS29JT, United Kingdom
[3] Department of Chemical Engineering, IIT Roorkee, Roorkee, 247667, India

KEYWORDS: Printed Circuit Boards (PCBs); Deep Eutectic Solvent (DES); Metal extraction; Kinetics; DFT calculations.

ABSTRACT

Waste PCBs the core of e-waste is rich in copper, tin, zinc, iron, and nickel. Leaching base metals from PCB used to be done in toxic, corrosive acidic/alkali mediums. In this work, an environmentally friendly method for leaching metals from thermally treated PCBs (TPCBs) of mobile phones was proposed using choline chloride based deep eutectic solvents (DES). DES selectivity and solubility of metals from metal oxides were the main screening criteria. FA-ChCl had the maximum solubility of Cu, Fe, and Ni, while Urea-ChCl had high Zn selectivity and solubility. Oxalic acid has high selectivity for Sn. FA-ChCl extracted Cu and Fe best at 16 h, 100 °C, and 1/30 g/mL. Urea-ChCl extracted Zn (90.4 ± 2.9%) from TPCBs at 100 °C, 21 h, 1/20 g/mL, and 400 rpm. Oxalic acid (1M) removed 92.3 ± 2.1% Sn from TPCBs in 1 h at 80 °C and 1/20 g/mL. The shrinking core model-based kinetic investigation of FA-ChCl for Cu extraction showed a diffusion-controlled process. The proposed method is greener than mineral acids utilized for metal extraction.

GRAPHICAL ABSTRACT

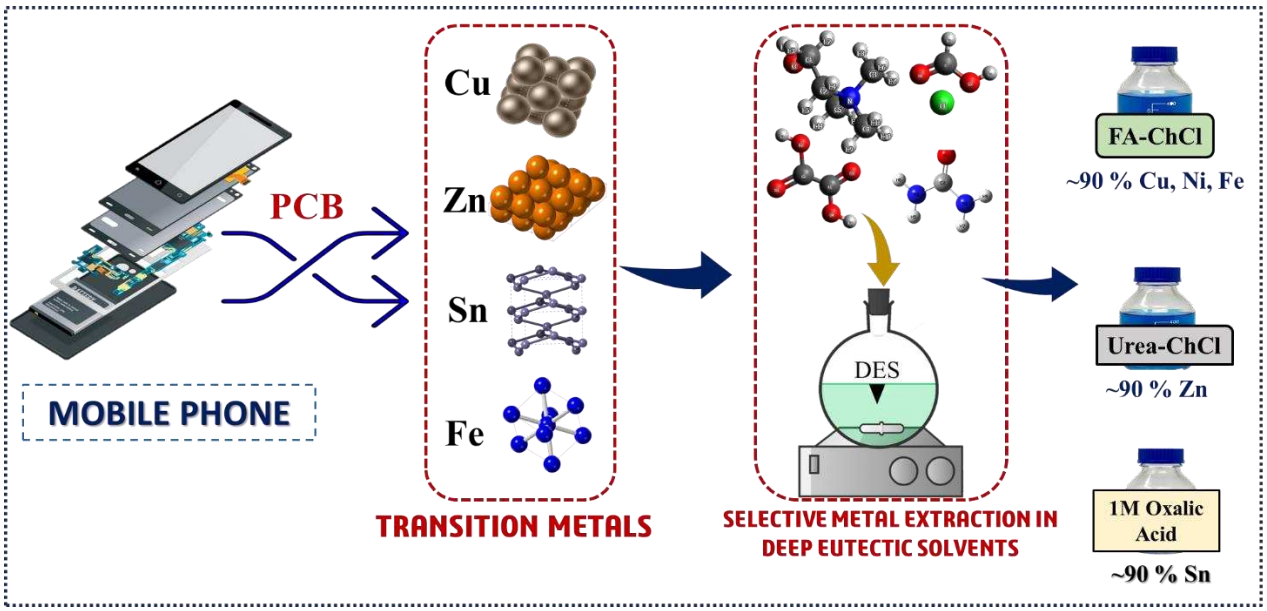

1. Introduction

Electronic waste (e-waste) is a vastly underutilized resource that offers a plethora of economic opportunities. E-waste contains a wealth of precious metals (platinum, gold, silver), base metals (aluminum, iron, copper), heavy (zinc, mercury, chromium, lead), and rare earth metals (tantalum, platinum groups) [1]. In 2019, the estimated value of treasured metals in e-waste such as gold, copper, iron, etc., inclusive of plastics obtained from e-waste, is assessed to be equivalent to USD 57 billion [2]. According to the UN World Economic Forum in 2019, the gold present in a tonne of e-waste is 100 times more valuable than 1 tonne of gold ores [2]. Likewise, a metric ton of printed circuit board (PCB) contains 30 to 40 times higher copper than one metric ton of natural copper ore [3]. The use of e-waste as a rich secondary source of metals can significantly bridge the huge gap between demand and supply of several scarce metals, e.g., tin, silver, gold, platinum, lithium, etc. The Global E-waste Monitor Report 2020 revealed that ca. 53.5 million metric tons (MMT) of e-waste was generated globally in 2019 [2]. The report also predicts that an astounding 74 MMT of e-waste will be generated by the year 2030, nearly double the amount generated 16 years ago [2]. Nevertheless, the recycling rate of e-waste is quite low and mostly concentrated in unregulated informal sectors, often involving open dumping or burning [4]. Metal extraction from e-waste presents opportunities in the context of a circular economy driven by the need to recycle valuable metals from discarded electronics and reduce environmental impacts from traditional virgin mining. Printed circuit boards (PCBs) are one of the vital components of any electronic gadget, constituting 3 % of the total collected electrical and electronic waste globally [5]. Recycling PCBs is necessary for economic and environmental reasons, as they are rich in valuable metals such as copper, iron, gold, silver, and hazardous metals such as lead, chromium, etc. PCBs are often referred to as an "Urban Mineral Source" due to their metal concentration being 10 times richer than that of ores [6].

The development of a metal recycling process from PCBs is necessary for the electronics industry to thrive sustainably. Conventional methods, such as electrostatic separation [7], froth floatation [8], and vibration gas-solid fluidized bed [9], have been used to separate distinct non-metallic and metallic fractions. Furthermore, to recover metals from e-waste, pyrometallurgy, hydrometallurgy, and biohydrometallurgy have been employed [3]. Pyrometallurgy operates at very high temperatures and produces hazardous gases like dioxins due to the presence of brominated flame retardants, (hydro)chlorofluorocarbons, and mercury in PCBs [10]. Hydrometallurgy, a flexible alternative approach for recovering metals, uses alkaline [11], cyanide [12], thiosulphate [13], mineral acid [14], etc., as leaching agents to extract metals such as copper, zinc and gold. However, poor selectivity, toxicity [15], and severe environmental threats have led to an exploration of greener alternatives to conventional metal extraction techniques [16].

The replacement of toxic reagents with green solvents, such as ionic liquids and supercritical fluids, has been proposed by several researchers [17]. Xiu et al. used supercritical water with HCl leaching for 100% Cu recovery and iodine-iodine leaching to recover silver, gold, and palladium from PCBs [18]. Golazary et al. combined the supercritical water process as pre-treatment followed by supercritical CO_2 to recover 97 % copper from PCBs at 60 °C and 200 bar [17a]. However, high pressure to attain the supercritical state is a concern in these technologies. Ionic liquids are promising and environmentally sound alternatives to organic solvents. Huang et al. used [bmim]HSO_4 ionic liquid with hydrogen peroxide to extract copper from PCBs [19]. Barrueto et al. observed that acidic ionic liquid ([Bmim]HSO_4 and [Hmim]HSO_4) extracted 86.2 % and 76.6 % copper, respectively, while basic ionic liquid ([Bmim]Cl) extracted 47.3 % silver and 19.1 % gold [20]. Nevertheless, the exploration of safer, cheaper, and tunable solvents for sustainable chemicals has received much attention in recent years.

Deep eutectic solvents, composed of naturally occurring compounds, have high extraction efficiency for metals and low toxicity with a cutting edge over ionic liquids in terms of easy preparation method, less corrosive, and relatively easy biodegradation. The advantage of DESs lies in the difference in the coordination ability of components and metals, providing a low-cost green strategy with the potential to selectively extract metals on a large scale from complex ores or waste material. Malonic acid-choline chloride (MA-ChCl), Oxalic acid-choline chloride (OA-ChCl), and Ethylene glycol-choline chloride (EG-ChCl) DESs were checked by Abbott et al. for transition metal oxide dissolution [24]. Selective dissolution of metals was observed in choline chloride (ChCl) DES. Since then, the development of DES synthesis has taken precedence in the sector as a means of effective metal extraction from complicated compounds under benign conditions [25]. Choline chloride-based DESs were reported to have highly efficient metal leaching from Li-ion batteries 26, 27, NdFeB magnets [26], ores [27], minerals [28], and electric arc furnace dust [29].

Recoveries of metals from spent lithium-ion batteries are extensively studied [30]. Li et al. found DESs to be a greener alternative to inorganic acids with metal leaching efficiency (>99 %) but with slower leaching kinetics [30c]. Wang et al. concluded that the high reducing power of Urea-ChCl DES makes it the best DESs for cathode recycling of Li-ion batteries [31]. Tran et al. observed that ethylene glycol-ChCl DESs recover 99.3 % of cobalt and lithium from lithium cobalt oxide, and metal leaching efficiency increases with time and temperature [30e]. The use of green solvents for metal extraction from e-waste is a promising area of research with the potential to reduce the environmental impacts of traditional mining processes. Lactic acid-ChCl [32], malonic acid-ChCl [32], and ethylene glycol-ChCl [33] have been used to extract metals from WPCBs, covering limited aspects. However, no detailed study of formic acid-choline chloride and urea-choline chloride in metal extraction from WPCBs has been done in the past to the best of our knowledge. Considering this research gap

and the Choline chloride DES advantage of selective metal extraction, the present study is proposed.

The present study uses green deep eutectic solvents and organic acid for the selective recovery of Cu, Fe, Ni, Zn and Sn from PCBs. Screening of green solvents was done in the first stage by dissolving various metal oxides [25b, 34]. Further, based on the solubility of metals in respective DESs, each selective solvent was chosen for optimizing parameters in metal extraction. FA-ChCl showed the highest solubility of Cu, Fe, and Ni, while Urea-ChCl exhibited selective solubility of Zn. For Sn extraction, 1M oxalic acid demonstrated the highest efficiency. TPCBs of mobile phones with high metal concentrations have been used as feed materials for metal leaching experiments in the screened solvents. The influence of several leaching parameters such as time, temperature, and S/L ratio, in base metal leaching in DESs has been discussed in detail. Since copper has the highest contribution to the metallic composition of PCBs, the shrinking core model leaching kinetics of the highly extracted copper using FA-ChCl DES, and the activation energy of copper were assessed. A plausible mechanism was proposed based on literature, DFT and Pourbaix diagram.

2. Materials and Methods

2.1. Chemicals and Reagents

Waste PCBs of miscellaneous brands used in this study were provided by Exigo Recycling Pvt. Ltd, Haryana, India. The PCBs were crushed and ground to a size below 1.0 mm for the experiment. For the digestion of solid samples, nitric acid (86 %, HNO_3) and hydrochloric acid (37 %, HCl) from Fisher Scientific were used to prepare the aqua regia solution.

For DES synthesis, choline chloride (> 98 %) was purchased from Alfa Aesar, formic acid (99 %), urea (> 98 %), ethylene glycol (> 95 %), malonic acid (99 %), and oxalic acid (99.5 %) were obtained from Fisher Scientific. Metal oxides, including copper oxide (> 99 %, CuO), iron oxide (> 96 %, Fe_2O_3), zinc oxide (> 97 %, ZnO), and nickel oxide (≥ 99 %, NiO) were purchased from Sigma Aldrich. For dilution, double-distilled water with a conductivity

of less than 1 µS/cm was employed. All the reagents used in this experiment are of analytical grade and were used as received.

2.2. Experimental

Waste PCB samples were comminuted and screened to obtain a powder with a particle size of less than 1 mm. Particles smaller than 1 mm in size were separated using an ASTM E11 # 18 mesh screen (American Society for Testing and Materials). The organic content was removed from the PCBs using thermal pre-treatment, which involved pyrolyzing them in an inert environment. Pyrolysis was conducted in a fixed bed reactor at 500 °C for 30 min in a nitrogen atmosphere, as these conditions are sufficient for the cracking of the plastic part of PCBs, as discussed by Marco et al. [35]. The extraction efficiencies of Cu, Zn, and Sn from TPCBs were calculated using the following formula (1).

$$Extraction\ efficiency\ (E\ \%) = \frac{C_l \times V_l}{Wm_{TPCB}} \times 100 \qquad (1)$$

Where C_l is the metal content in leached solution (g/L); V_l is the leach volume (L), and Wm_{TPCB} is the weight of the metal in TPCBs (g).

2.2.1. Synthesis of Deep Eutectic Solvents

The DESs were prepared via the heating method. Hydrogen bond acceptor (HBA), ChCl, was combined with hydrogen bond donors (HBD), i.e., FA, urea, ethylene glycol, malonic acid, and oxalic acid in a (2:1) molar ratio in sealed 50 mL glass vials while being continuously stirred at 200 rpm at 50°C to create a eutectic mixture. However, mole ratios of individual components in OA-ChCl and MA-ChCl DES were 1:1 [25a]. The solvents were then stored at room temperature in a desiccator to avoid moisture absorption.

2.2.2. Metal leaching

All leaching/ extraction experiments were carried out in 50 mL Borosil glass on a hot magnetic stirrer (Cole-Parmer Stuart) with an oil bath. Primarily, for screening DESs, 0.1 g of

167 respective metal oxides: CuO, Fe_2O_3, ZnO, and NiO were dissolved in 10 mL EG-ChCl,
168 Urea-ChCl, FA-ChCl, OA-ChCl, and MA-ChCl for 24 h at 80 °C. The temperature of 80 °C
169 is selected as Abbott et al. [34] observed high solubility of zinc in urea-ChCl at a temperature
170 greater than 60 °C. Respective DES were selected for individual metal extraction. 1 M oxalic
171 acid was also tested to check the solubility of copper, iron, zinc, and nickel from oxides.

172 A parameter selectivity (S_m) was defined to evaluate the effectiveness of different leaching
173 solutions. It is calculated by dividing the concentration of the metal of interest (m) by the sum
174 of concentrations of all leached metals in the solution by equation (2).

175 $$S_m = C_m / \sum_i C_i \times 100\ \% \qquad (2)$$

176 Here, C_m is the concentration of metal of interest in leaching solution and C_i is the
177 concentration of any metals in a leached solution.

178 A series of leaching optimization experiments were conducted to find the maximum copper,
179 zinc, and tin leaching efficiency in their respective highest soluble solvents. Filter paper with
180 a 0.22 µm pore size was used to separate the solid residue from the leach liquor. The residue
181 was washed with ultrapure water and dried for 24 h at 100 °C. For metal extraction from e-
182 waste, 1 g of TPCB sample was taken in a given volume of FA-ChCl, Urea-ChCl, and 1M
183 oxalic acid solution. The effect of time (1-32 h), temperature (20-100 °C), and S/L ratio
184 (1/10-1/40 mg/L) were evaluated for Cu, Fe, Zn, Ni, and Sn in FA-ChCl. In Urea-ChCl, the
185 temperature was varied from (20-140 °C), stirring speed (100-800 rpm), time (1- 24 h), and
186 S/L ratio (1/10-1/50 g/mL). The extraction of tin in oxalic acid time was evaluated at process
187 conditions with time (1-5 h); temperature (50-80 °C) and oxalic acid concentration 0-3 g/L.
188 High temperatures (>100 °C) were avoided considering the economical and energy point of
189 view [36]. Glass bottles were closed to prevent the loss of vapors.

190

2.2.3. Individual recovery of copper

The metal-leached solution obtained under optimized conditions was utilized for copper recovery from FA-ChCl through the cementation process. The metallic zinc powder was introduced into the leached solution to facilitate the recovery of metallic copper. The process began by transferring 200 mL metal leached solution into a beaker followed by the gradual addition of Zn powder. The appropriate stoichiometric amount of Zn was used to ensure effective copper cementation. Once the cementation was completed, the precipitated copper was recovered, dried, and subjected to analysis. The concentration of metal ions in the solution is determined by ICP-MS and cementation efficiency (θ) was calculated by equation *(3)*:

$$\theta = (1 - \frac{C}{C_0}) \times 100\,\% \quad (3)$$

Here, θ is metal precipitation efficiency (%), C_0 is initial metal concentration in optimized leaching solution, mg/ L; and C is metal concentration in a solution after cementation, mg/L.

2.3. Instrumentation and analysis

A Nicolet iS50 FTIR spectrophotometer with an ATR crystal detector was used to record infrared spectra. Samples were scanned 32 times with a resolution of 4 cm^{-1} in the range of 400-4000 cm^{-1}. Background reference spectra were obtained before sample measurement to avoid interferences. All samples were measured under atmospheric conditions.

The distribution of metal phases was investigated using X-ray diffraction (XRD) by Rigaku Mini Flex 600 instrument from Japan. Cu-K radiations were utilized, with graphite serving as a monochromator. The XRD measurements were conducted at 40 kV and 15 mA, employing an X'Celerator detector. The scanning process involved a ramp rate of 5°/min, spanning an angle range of 5-80°.

Netzsch STA449 Thermo Gravimetric Analyzer (TGA) was used to assess the thermal degradation of DES. 10–20 mg of DES was placed in a nitrogen environment throughout a temperature range of 25–800 °C.

The density of solvents was measured by Mettler Tolardo DE45 Delta Range Density meter. The viscosity of DESs was measured by Anton Paar MCR302 rotational and oscillatory rheometer equipped with cone and plate geometry (CP 50, diameter 50 mm, and angle 1°) at 303.15, 323.15 and 343.15 K temperatures at constant shear rate of 1000 s^{-1}.

Metal extraction in DESs was determined by Elan DRCe (Perkin Elmer) ICP-MS, diluting the samples 1000 times with doubly distilled water. The solubility experiments and measurements were done in triplicate.

2.4. Computational Method

A theoretical study of DES was done by optimizing ChCl, FA, urea, and oxalic acid. Geometrical optimization of structures was done using Gaussian with B3LYP 631 g+ (d,p) basis set [37]. The dispersion effect was avoided by adding the keyword "empirical dispersion=D3" in the command section. Hydrogen bond distances and angles of DESs have been calculated and quantified for H-bonds. The spatial distribution of electrostatic interactions in the solvent system was determined by Electrostatic potential surface (ESP) calculation. The interaction energy of copper with hydrogen bond donors of DES has been assessed.

3. Results and Discussion

3.1. Characterization of PCB and TPCB

As a feedstock, PCBs are rich in critical metals such as Cu, Ag, Au and Al. Table 1 summarizes the elemental composition of the PCB used in the current study. Among these metals, Cu is the most prevalent metal in the PCB constituting 29.6 wt%, (see Table 1). After

subjecting the PCB to the thermal treatment, the Cu content increased to 58.8 wt% due to the removal of the non-metallic fraction. The initial Fe and Zn contents in the PCB were 9.6 wt% and 0.2 wt%, respectively, and were enriched to 14.4 wt% and 0.5 wt% in the TPCBs. Additionally, the contents of Al, Ni and Sn ranged from 0.4-2 wt%, in the PCBs, and enriched to 0.6-8 wt% in the TPCBs [38]. The concentrations of transition metals in the PCBs are comparable to those previously reported [38].

Figure 1 compares the FTIR spectra and XRD patterns of the PCB and TPCB. The FTIR spectra (Fig. 1a) of the PCB show the presence of CH_3 methyl aromatics at 2967 cm^{-1}, C=O at 1738 cm^{-1}, benzene ring at 1610 cm^{-1} and 1506 cm^{-1}. C-Cl and C-Br functional groups in the range of 500-750 cm^{-1}. In the case of TPCB, several characteristic peaks of PCB (C=O, halogens, C=C trans) disappeared, signifying the loss of the organic functional group after pyrolysis at 500 °C.

Table 1. Elemental composition of PCB and TPCB (w/w%).

	Cu	**Fe**	**Al**	**Zn**	**Ni**	**Sn**
PCB	29.63 ± 1.25	9.66 ± 0.20	0.43 ± 0.02	0.15 ± 0.01	1.26 ± 0.12	1.90 ± 0.14
TPCB	58.76 ± 2.01	14.45 ± 1.20	0.62 ± 0.03	0.52 ± 0.02	2.53 ± 0.13	7.88 ± 0.17

Figure 1b compares XRD patterns for PCB and TPCB showing peaks at 44°, 51° and 74°, which correspond to metallic copper with Miller Indices (111), (002) and (022), respectively (JCPDS 00-004-0836). As such, the pyrolysis process does not affect the metal phase or its oxidation state. Figure 1c depicts the models of HBD involved in this study.

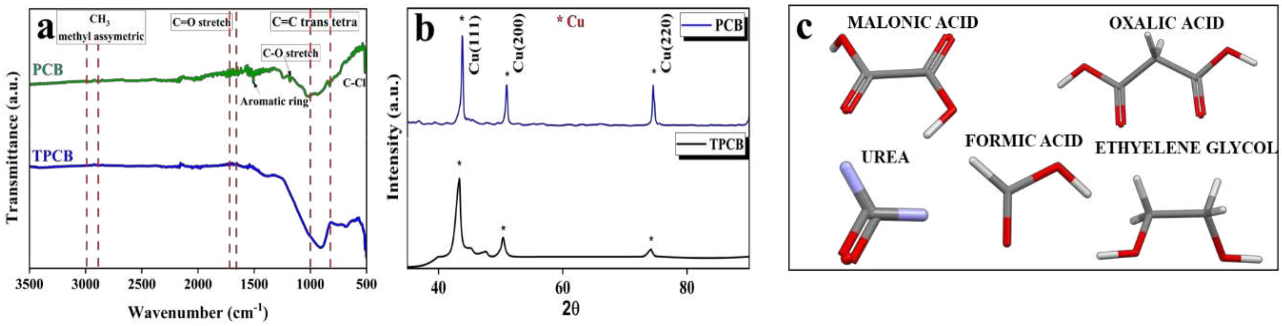

256

257 **Figure 1.** FTIR of PCB and TPCB (a); XRD of PCB and TPCB with clear peaks (*) at 44°,
258 51° and 74°. (b); models of HBDs used in the DES (c).

259

260 **3.2. Screening of DES and strategies for metal extraction:**

261 To determine the DES for maximum extraction of Cu, Ni, Fe, Zn and Sn, the respective metal
262 oxides were tested for dissolution in a range of DES: EG-ChCl, Urea-ChCl, FA-ChCl, OA-
263 ChCl, MA-ChCl, and 1M oxalic acid, as shown in Table S1.

264 The solubility of Cu in FA-ChCl was 1.60 ± 0.06 ($\times 10^5$) ppm. However, this DES had the
265 lowest solubility of Zn at 3.12 ± 0.12 ($\times 10^2$) ppm, while OA-ChCl and MA-ChCl had much
266 higher solubilities for Zn at 9.65 ± 0.09 ($\times 10^4$) ppm and 1.62 ± 0.05 ($\times 10^4$) ppm, respectively.
267 For Cu, those DESs showed an intermediate solubility, which affects its selectivity towards
268 zinc. The solubility of Zn in Urea-ChCl was in the range of 10^5 ppm, but for Cu, the
269 solubility was very low at 10 ppm. Based on these findings, FA-ChCl was selected to extract
270 Cu from TPCB, and Urea-ChCl for Zn extraction.

271 As for Sn, SnO_2 solubility in dicarboxylic acid DES was higher as compared to other types of
272 DES. OA-ChCl DES also leached Cu and Zn in the solution due to the presence of Cl^-.
273 Oxalic acid is a good reducing agent, consequently having a high selectivity for Sn over Zn
274 and with a high leaching efficiency (> 95 %) [39]. This high selectivity results from the
275 interaction of 2 carbon atoms of oxalic acid, preferentially interacting with stannous salt (Sn
276 salt) to form a Sn-dicarboxylate complex [39-40]. Furthermore, TPCB is taken as the feed

material to identify trends in selectivity and explore the leaching behavior of solvents under the same experimental conditions as the metal oxides at 80 °C, as shown in Figure 2 and elaborated in Table S1.

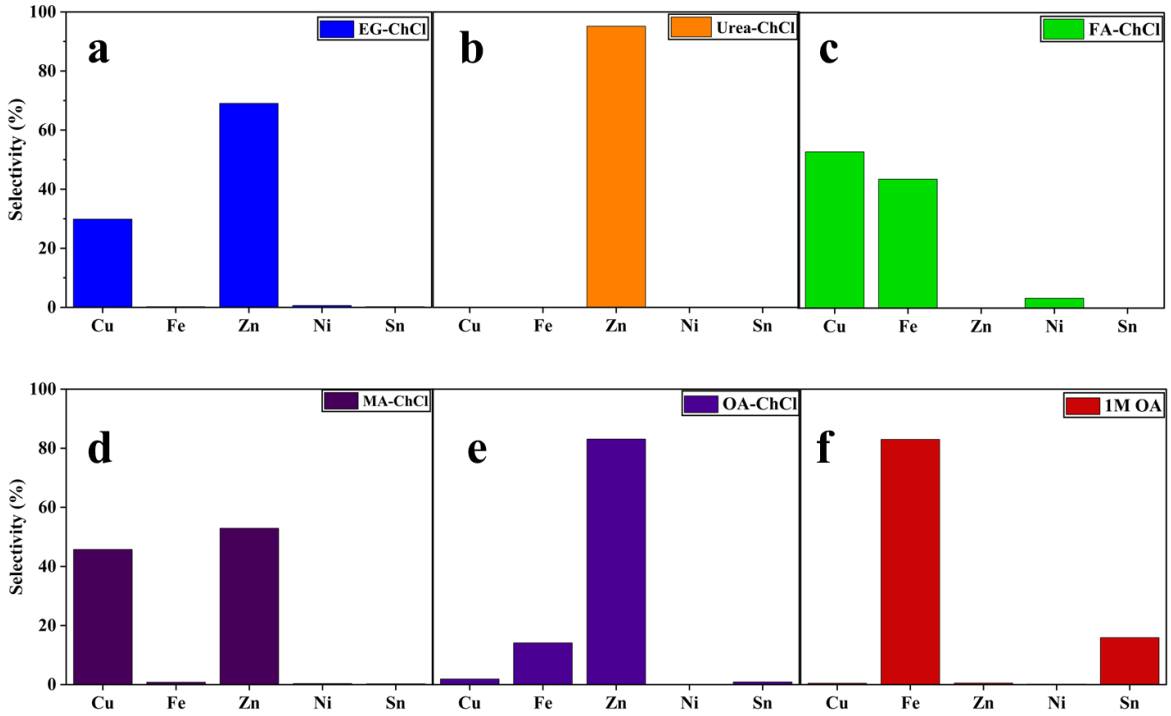

Figure 2. Selectivity of leached metals into different DESs and oxalic acid

3.3. Characterization of DES

The physicochemical properties of DES are obligatory for its industrial applications. The synthesized DES, including FA-ChCl, EG-ChCl, MA-ChCl, and OA-ChCl, were characterized to estimate their physical properties, including the density, viscosity, and conductivity of DES. These properties have significant implications for understanding fluid behavior, heat transfer, mass transport, and designing chemical processes [21]. Density and viscosity were evaluated at different temperatures to comprehend the behavior of the liquid under various thermal conditions.

Choline chloride DES typically has a density of 1-1.3 g/cm^3. [41]. In our last study, the densities of FA-ChCl, MA-ChCl, and OA-ChCl were reported to be 1.16, 1.23 and 1.15,

292 g/cm^3, respectively [41]. The density of ethylene glycol-choline chloride was 1.08 g/cm^3 [42].
293 The shear viscosities of all the synthesized DES were measured at 30, 50 and 70 °C, to
294 understand the behavior of solvent viscosity with temperature according to Table 2. The
295 viscosity of FA-ChCl ranged from 0.4 to 1 mPa.s across the temperature range, which was
296 significantly lower than the viscosity of Urea-ChCl, which was several hundred mPa.s.
297 Consequently, FA-ChCl DES exhibits little mass transfer resistance compared to Urea-ChCl.
298 The high viscosity of Urea-ChCl can be attributed to factors such as the presence of a
299 prevalent hydrogen bond network, large ion size, and small void volumes. For both DES the
300 fluid viscosity decreased with increasing temperature, see Table 2 [22]. Higher temperatures
301 also enhance the leaching efficiency by enhancing the mass transfer of the dissolved species
302 [43]. In the context of extracting metal ions from electronic waste, it is often observed that a
303 reduced viscosity of the leaching agent, such as DES, is advantageous for facilitating the
304 dynamic conditions of the liquid-solid reaction and the subsequent separation process.

305 Figure 3a shows the IR spectra of FA, ChCl and 2FA-ChCl. Vibrations of FA-ChCl account
306 for OH stretching at 3359 cm^{-1}, C-H stretching at 1474 cm^{-1}, sp^2 C-O stretching at 1710 cm^{-1},
307 and sp^3 C-O stretching at 1078 cm^{-1} [44]. The C-H vibration shifted from 1482 cm^{-1} in ChCl to
308 1474 cm^{-1} in FA-ChCl. FA-ChCl exhibits significant peaks of neat FA and ChCl peaks with
309 some shifts indicating an H-bond in between FA and ChCl.
310 Figure 3b represents the IR spectra of ChCl, urea and Urea-ChCl. The IR spectra of urea
311 show symmetric stretching C=O at 1675 cm^{-1}, which was also observed in DES with a shift
312 to 1665 cm^{-1}. The frequency of 1590 cm^{-1} in urea represents symmetric bending NH and NH_2,
313 which was observed at 1599 cm^{-1} in Urea-ChCl. NH stretch peak of urea at 3433 and 3342
314 cm^{-1} has a lower shift to 3322 cm^{-1} and 3186 cm^{-1} in Urea-ChCl, which is attributed to the N-
315 H stretch. It should be noticed that the Urea-ChCl characteristic spectrum nearly overlaps that

of urea and ChCl. CH_3 at 1482 cm^{-1}, CH_2 at 1084 cm^{-1}, and CCO at 950 cm^{-1} appeared in the DES spectrum, revealing that the structure of ChCl was retained in DES.

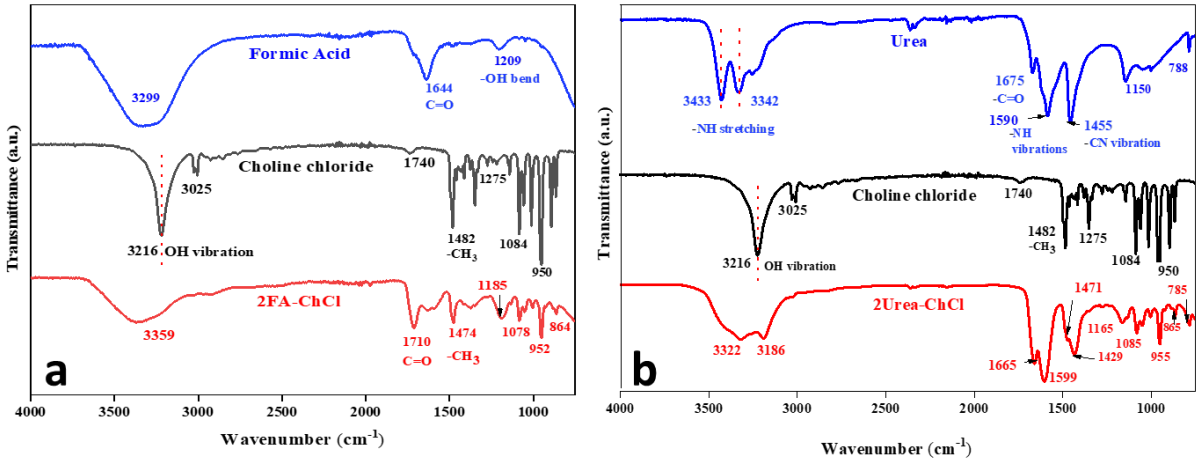

Figure 3. FTIR of FA, ChCl and 2FA-ChCl (a); Urea, ChCl and 2Urea-ChCl (b).

The thermal stabilities of FA-ChCl and Urea-ChCl were evaluated using TGA. FA-ChCl degrades from 388 K, while the degradation temperature is much higher for Urea-ChCl at 440 K. Therefore, the maximum operating temperature of FA-ChCl should be less than 388 K, whereas, for Urea-ChCl, 440 K is the maximum operating temperature, as depicted in Figure S1.

Table 2. Viscosity (mPa.s) of the synthesized DES as a function of temperature.

DES	30 °C	50 °C	70 °C
FA-ChCl (2:1)	1.04 ± 0.001	0.54 ± 0.002	0.46 ± 0.001
Urea-ChCl (2:1)	725 ± 13.100	160 ± 2.100	99 ± 4.280

3.4. Parameter study on metal extraction

3.4.1. Effect of oxidizing agent

DES have no oxidizing power of their own [45]. However, they could be used to dissolve metals either using oxidizing agents or as an electrolyte for the electro-oxidation of metals [45]. Without the addition of oxidizing agents, there is a slight elemental metal breakdown from e-waste into the solution, specifically in DES. A further oxidation phase with an oxidizing agent is therefore required for the dissolution of metals. Potassium permanganate

($KMnO_4$) and hydrogen peroxide (H_2O_2) are commonly used oxidizing agents for the oxidation of metals in the leaching system. In this system, both $KMnO_4$ and H_2O_2 were tested in combination with DES to extract metals. The addition of $KMnO_4$ in DES showed higher dissolution of copper and iron as compared to H_2O_2, as shown in Table S2. However, potassium permanganate can be relatively expensive and generate significant amounts of waste, making it less desirable in applications. Hence, the mild oxidizing agent hydrogen peroxide was selected for further experiments.

Different molar concentrations of H_2O_2, ranging from 0.5 M – 2 M, have been investigated to examine the impact on metal extraction while keeping other parameters constant (400 rpm, 24 h, 1/20 g/mL, 100 °C). After adding H_2O_2, metal extraction in FA-ChCl increases to 94.3 ±2 % Cu, 81.2 ±2.4 % Fe and 91.6 ±1.1 % Sn as depicted in Figure 4. There was no significant change in metal extraction beyond 1M H_2O_2 in FA-ChCl DESs. Thus, 1M is chosen as the optimum H_2O_2 concentration. Hydrogen peroxide has a similar effect as the presence of oxygen; the extra oxygen is known as "active oxygen," which interacts with metals and changes their oxidation states. Moffett et al. discussed the mechanism of oxidation or reduction reaction of H_2O_2 with Cu(II) and Fe(III) [46]. Colcleu et al. illustrated the interaction of H_2O_2 with metallic copper in the presence of sulphuric acid [47]. Equation (4-6) discusses the credible mechanism of metal oxidation.

$$M\,(s) \rightarrow M^{2+} + 2e^- \qquad (4)$$

$$H_2O_2\,(aq) + 2\,H^+(aq) + 2e^- \rightarrow 2\,H_2O \qquad (5)$$

$$M + H_2O_2\,(aq) + 2\,H^+ \rightarrow M^{2+} + 2\,H_2O \qquad (6)$$

Furthermore, the oxidized metal forms complexes either with Cl^- or with -COOH of DESs, which enhances the efficiency of metal extraction. There have been almost negligible studies on the extraction of metals from electronic waste using DESs with H_2O_2. However,

carboxylic acids were used as a leaching agent along with hydrogen peroxide to extract metals from electronic wastes [48]. For zinc extraction in Urea-ChCl, H_2O_2 was observed to have maximum extraction efficiency at 1M H_2O_2. The molar concentration of oxalic acid was varied from (0.5-2 M) to check the extraction of tin according to Figure 7a. It was observed that at 1 M, there is the maximum extraction of tin, and it remained the same on further increasing molar concentration. However, no oxidizing agent was used to leach tin from PCB using optimized 1 M oxalic acid.

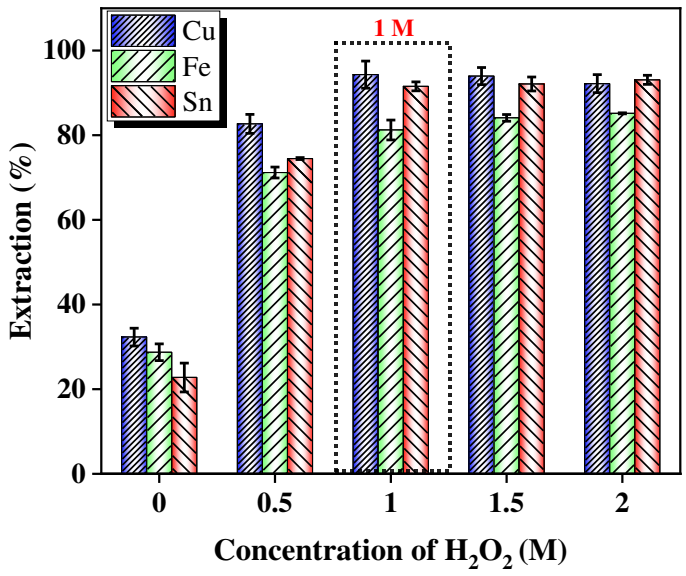

Figure 4. Effect of H_2O_2 concentration on metal extraction from PCB using FA-ChCl (400 rpm, 24 h, 1/20 g/mL and 100 °C)

3.4.2. Effect of temperature

Based on the thermal stability of solvents by TGA, the maximum operating temperatures were selected. The efficiency of metal extraction by changing reaction temperature was studied in the individual solvent system by ranging temperature from 20-100 °C for FA-ChCl, 20-100 °C for 1M Oxalic acid, and varying 20-130 °C for Urea-ChCl. For FA-ChCl, all the other parameters were kept constant, time at 21 h, solid-liquid ratio of 1/20 g/mL, and

stirring speed of 300 rpm. Figure 5b depicts that an increase in temperature had a remarkable effect on metal extraction efficiency from ~40-42 % of copper, nickel, and iron to greater than 90 % of metal extraction in FA-ChCl at 100 °C. An increase in reaction temperature enhances the collisions between reactants, thereby enhancing metal extraction [49]. The optimum temperature of 100 °C was selected for FA-ChCl.

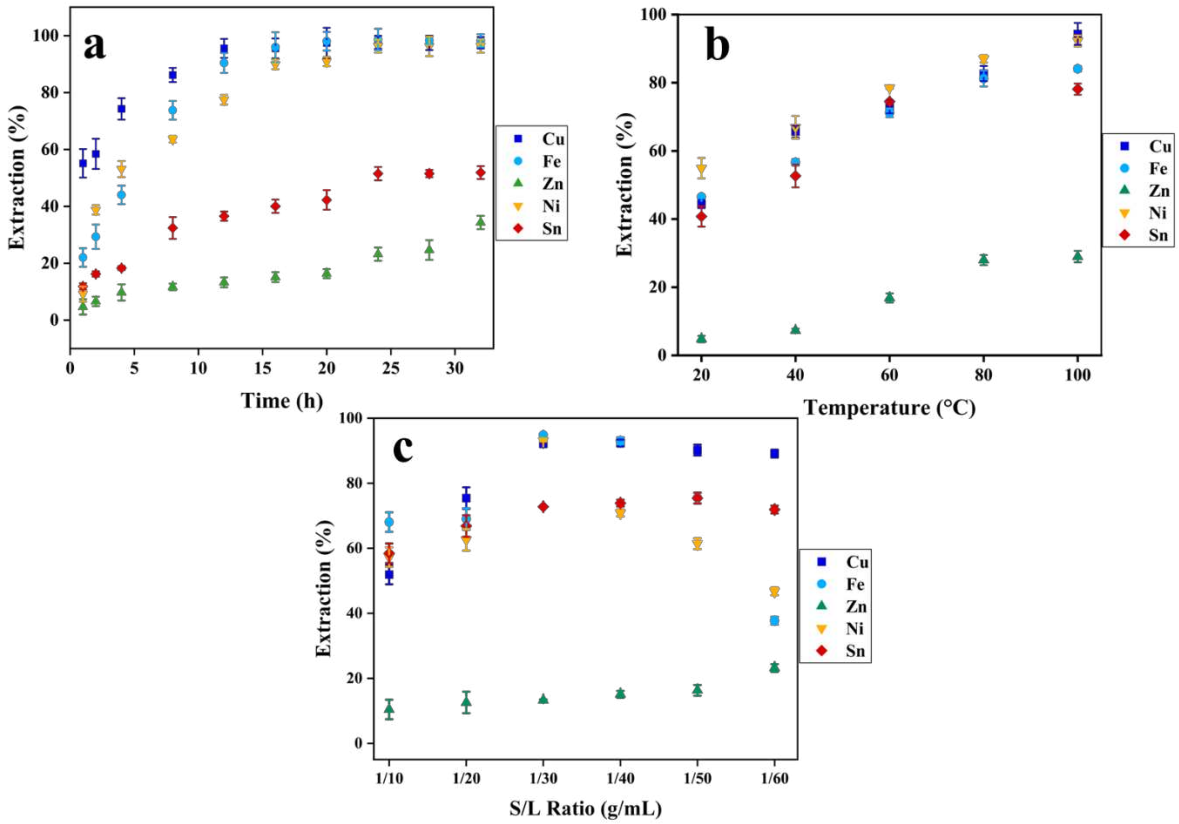

Figure 5. Effect of Time (100 °C; 1/20 g/mL; 300 rpm) (a); Temperature (21 h; 1/20 g/mL; 300 rpm) (b); S/L ratio (100 °C; 21 h; 300 rpm (c); in metal extraction from TPCB to FA-ChCl.

Low-moderate reaction temperatures (20-140 °C) were selected for Urea-ChCl to evaluate temperature effect on metal extraction efficiency, keeping other parameters viz, time (21 h), solid-liquid ratio (1/20 g/mL), stirring speed (300 rpm) constant. In Urea-ChCl, zinc extraction drastically increased to 90.37 ± 1.97 % on increasing temperature to 80 °C, as

shown in Figure 6a. In the temperature range between 80-120 °C, selective extraction of Zn was also observed. Therefore, 80 °C is preferred as the optimum temperature for Urea-ChCl. 1M oxalic acid was examined from 20-50 °C to evaluate the extraction of tin from TPCBs, as shown in Figure 7c. It was observed that extraction of tin at 20 °C was 75.32 ± 1.06 % while it raised to 91.28 ± 2.32 % at 80 °C in 1 h, 1/20 g/mL, 300 rpm.

3.4.3. Effect of time

The effect of metal extraction efficiency in individual DESs was studied by varying time from 1-32 h at 100 °C constant temperature and 1/20 g/mL in FA-ChCl. It was observed that copper, nickel, and iron extraction reached 93.5 ± 3.47 %, 90 ± 1.73 %, and 93.5±2.52 % extraction at 21 h and are almost at equilibrium after 21 h. After 24 h, the extraction efficiency of these three metals in FA-ChCl was above 93 %, as demonstrated in Figure 5a. However, low soluble metals zinc and tin reach 34.3 ± 2.34 % and 51.8 ± 2.27 % metal extraction till 32 h, respectively, in FA-ChCl.

The effect of time on metal extraction in Urea-ChCl was studied by varying it from 1-24 h at (100 °C; 1/20 g/mL; 400 rpm). It was observed that after 16 h, zinc extraction was 90.1 ± 4.1 % and did not have significant changes in metal extraction, as shown in Figure 6b. Hence, 16 h is the optimum time for maximum Zn extraction.

The time effect on metal extraction from PCBs with oxalic acid was studied from 30 min to 2 h, as shown in figure 7b. Temperature of 100 °C, S/L ratio of 1/20 g/mL, and 300 rpm were fixed. It was observed that in 1h, extraction of tin was 91.3 ± 2.1 % which varies barely on increasing time till 5 h. Therefore, 1h is chosen as the optimum time for maximum tin extraction.

3.4.4. Effect of S/L ratio and stirring speed

Metal extraction efficiency in DES is highly dependent on the available area per unit volume of the solution. The solid-liquid ratio was examined in FA-ChCl for metal extraction, ranging from 1/20 to 1/40 g/mL while keeping other process parameters constant: time (16 h), temperature (80 °C) and stirring speed (300 rpm). It must be noted that along with DESs, 1M H_2O_2 has been used for metal leaching experiments in DES systems. It was observed that 1/30 g/mL is the optimum solid-liquid ratio for 94.5 ± 2% copper, 95.1 ± 1.2% iron, and 95.6 ± 1.8 % nickel extraction in FA-ChCl as shown in Figure 5c. At a higher S/L ratio (1/10 g/mL) there is a reduction in metal extraction due to the diminution of available surface area per volume of solution resulting in low interaction of PCB powder and FA-ChCl solution. Furthermore, at a low S/L ratio, there is an increase in solution viscosity due to the agglomeration of PCB powder particles, which is unfavorable for mass transfer and diffusion resulting in low metal extraction [43]. On further decreasing the S/L ratio, there is an excessive solvent that does not have a significant effect on metal extraction efficiency [50].

In Urea-ChCl, zinc extraction reaches 90.1 ±1.1 % at a 1/30 g/mL ratio, with conditions of 100 °C, 21 h and 400 rpm stirring speed. Further, increasing the volume of solution only yields a marginal difference in extraction efficiency. Thus, a 1/30 solid-liquid ratio is considered the optimum condition for achieving maximum zinc extraction in Urea-ChCl, as shown in figure 6c. In the case of oxalic acid, after a 1/20 g/mL ratio, there was no significant difference in tin extraction as depicted in figure 7d; Wang et al. conducted selective extraction of tin from zinc leaching residue using oxalic acid-sulfuric acid mixture and concluded that a lower S/L ratio is beneficial for efficient mass diffusion from solid to liquid [51].

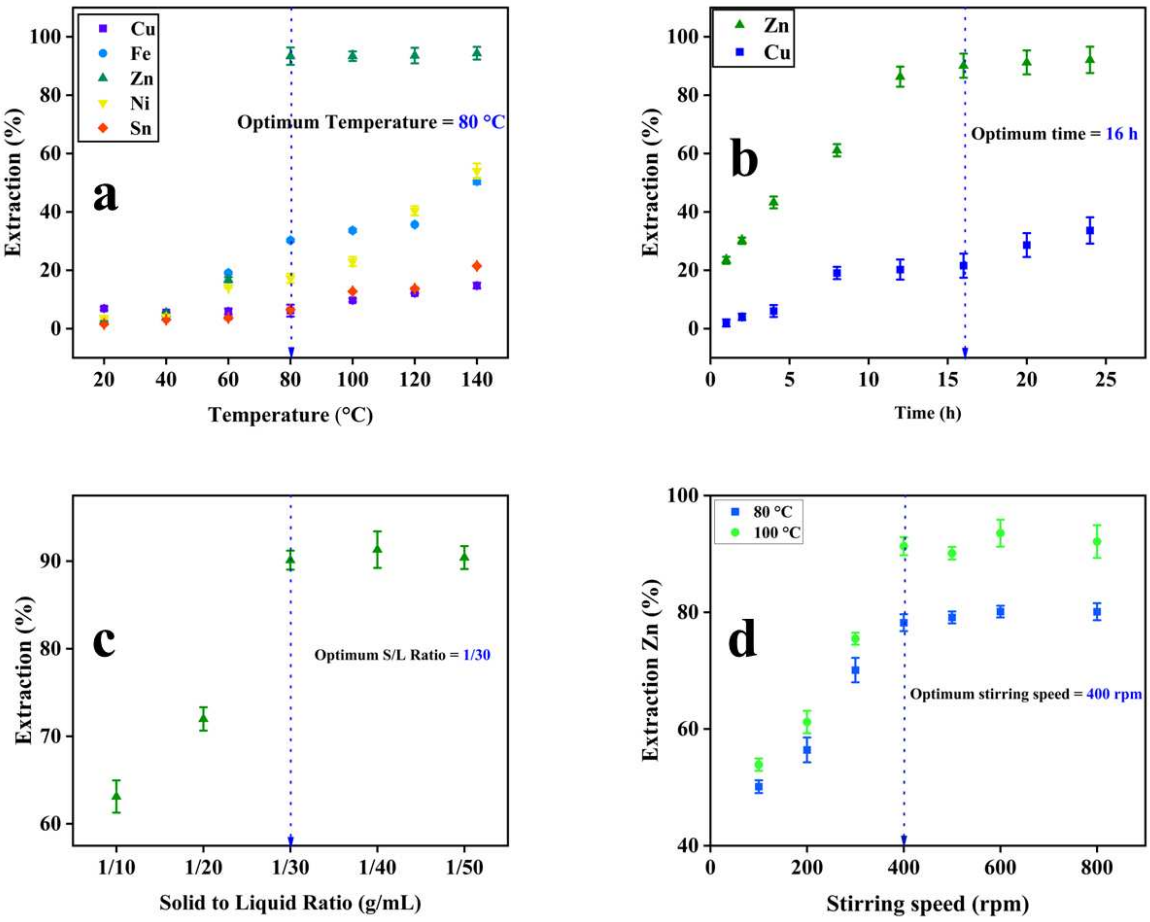

Figure 6. Effect of Temperature (21 h; 1/20 g/mL; 400 rpm) (a); Time (100 °C; 1/20 g/mL; 400 rpm) (b); S/L Ratio (100 °C; 21 h; 400 rpm) (c); and stirring speed (d) in metal extraction from TPCB in Urea-ChCl.

A high S/L ratio is required to increase process yield; however, it reduces metal extraction efficiency. Hence, there should be a trade-off between metal extraction efficiency and process yield. Thus, a 1/20 g/mL and a 1/30 g/mL ratio are the optimum solid-liquid ratios for maximum tin extraction in oxalic acid and base metals extraction in FA-ChCl, respectively.

In order to reduce the impact of external mass transfer, the effect of stirring speed was visualized by changing the stirring speed in extremely viscous Urea-ChCl DESs from 100 to 800 rpm, as shown in figure 6d. It was observed that 400 rpm is the optimum stirring speed for maximum zinc recovery. An increase in stirring speed leads to efficient mass transfer without agglomeration, thereby decreasing mass transfer resistance and increasing metal

447 extraction. However, 300 rpm is selected for FA-ChCl and oxalic acid as in literature, 300
448 rpm was found to be the optimum stirring speed [52].

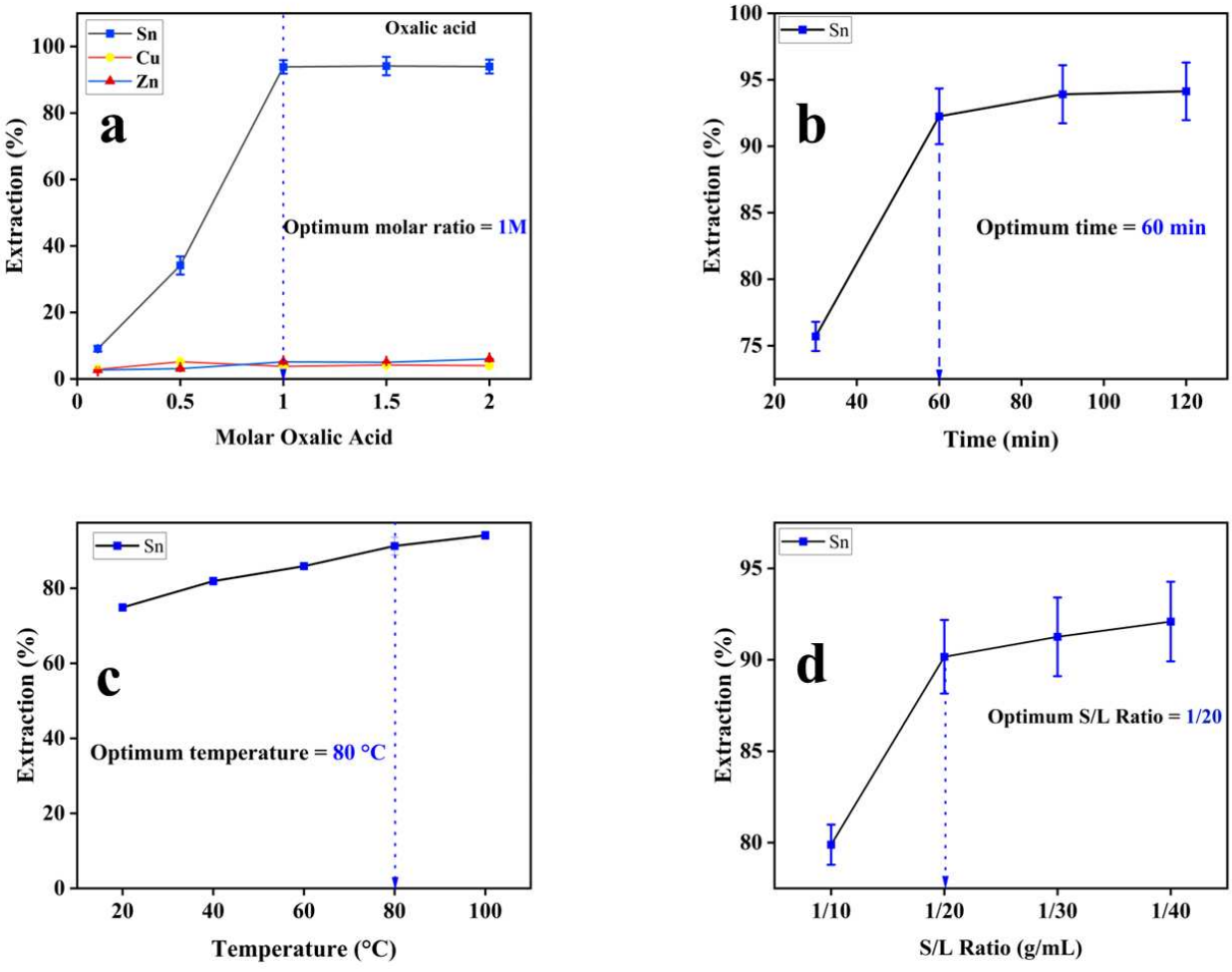

4

450 **Figure 7.** Effect of Molar concentration of oxalic acid (100 °C; 1 h; 1/30 g/mL) (a);
451 Reaction time (100 °C, 1/20 g/mL) (b); Reaction temperature (1 h; 1/20 g/mL) (c); S/L Ratio
452 (100 °C; 1 h) (d). stirring speed is constant= 300 rpm in oxalic acid.

453 **3.5. Kinetic study**

454 The dissolution of metals from PCBs to organic acid-choline chloride DES is a solid-liquid
455 reaction. Liquid goes through the solid with an effective diffusivity while solid was supposed
456 to homogeneously diffuse all over the material. In the present work, the reaction for metal
457 extraction begins at the particle's outer surface, which causes the reaction zone to contract as

the reaction time increases. Due to this, the reaction zone moves inward, and the extracted metals stay in the aqueous solution. There are two major assumptions of the shrinking core model. The first assumption is that the reacting solid particle has a spherical shape. This simplifies the mathematical description of the reaction because it allows for a uniform reaction rate at the particle's surface. Particles can have more complex shapes, but the spherical symmetry assumption is often used as an approximation[53]. The second assumption is that the rate of the chemical reaction at the surface of the solid particle is uniform[53]. As copper is a bulk metal, copper dissolution kinetics in FA-ChCl DESs are discussed in detail in this study. Metal leaching has three vital steps, which involve (1) Diffusion of reactants: molecules/ions (H^+, FA, Urea, Cl^-, etc.) into the solid surface of PCBs (Cu, Fe, Zn, Ni, Sn) and adsorbed (2) Interfacial surface chemical reaction by complexation reaction. (3) Diffusion of products: dissociation of the metal complex (Zn-Urea, Cu-Choline chloride, etc.) and diffusion in DES solution. As copper content in TPCBs is maximum, hence kinetics of copper extraction in FA-ChCl is discussed in detail. The process of metal extraction in organic acids involves the principle of complexation, where the organic acid forms a complex with the metal ions, which makes them more soluble in the aqueous solution. It can be implied from the abovementioned discussion that extraction of metals depends on mass transfer and chemical reaction on the surface.

Table 3. Kinetic parameters of interfacial chemical reaction controlled and diffusion-controlled models at different reaction temperatures.

Temperature (°C)	$\mathbf{1\text{-}(1\text{-}\chi)^{1/3}}$		$\mathbf{1-2/3\chi-(1-\chi)^{2/3}}$	
	k**(h^{-1})**	**R^2**	k**(h^{-1})**	**R^2**
20	0.01159	0.870	0.0029	0.958
40	0.01209	0.916	0.00404	0.975
60	0.01917	0.913	0.00848	0.988
80	0.01840	0.951	0.00851	0.972
100	0.02481	0.922	0.01169	0.977

Organic acids form complexes with the metal ions, and the resulting complexes are soluble in water, which facilitates their separation from the solid material and leaves an inert solid

residue without metals. The leaching process was analyzed using a kinetics model based on the shrinking core concept. This model was employed due to the observation that the solid surface underwent shrinkage during the reaction, resulting in the inward movement of the reaction zone and the manifestation of a shrinking core phenomenon. Within the leaching system, the step that exhibits the lowest rate is referred to as the rate-determining phase. The extraction process is diffusion controlled or chemical reaction controlled is denoted by equations (7-8)

$$1-(2/3)\,\chi-(1-\chi)^{2/3}=kt \quad \textit{(diffusion controlled)} \qquad (7)$$

$$1-(1-\chi)^{1/3}=kt \quad \textit{(interfacial chemical reaction controlled)} \qquad (8)$$

Here, χ is the leaching efficiency of metals (Cu), %; k is the rate constant, h^{-1}; t is time in h. Figure 8 (a-d) represents the experimental data fitting in the equations (7-8). It is evident from Figure 8 (b and c) that the extraction of copper in FA-ChCl fits well with equation 7 and is a diffusion-controlled phenomenon. The rate constants are determined in the temperature range of 20-100 °C using linear regression. The k value and R^2 are represented in Table 3, through which it can be concluded that R^2 of diffusion-controlled model $\mathbf{1-2/3\chi-(1-\chi)^{2/3}}$ is near to 1. Hence, in the extraction of Cu from PCBs to FA-ChCl, diffusion is a rate-determining step. The activation energy (E_a) for Cu extraction was regulated by a linearised form of the Arrhenius equation (9) and portrayed in Figure 8d.

$$ln\,k = ln\,A - \frac{E_a}{RT} \qquad (9)$$

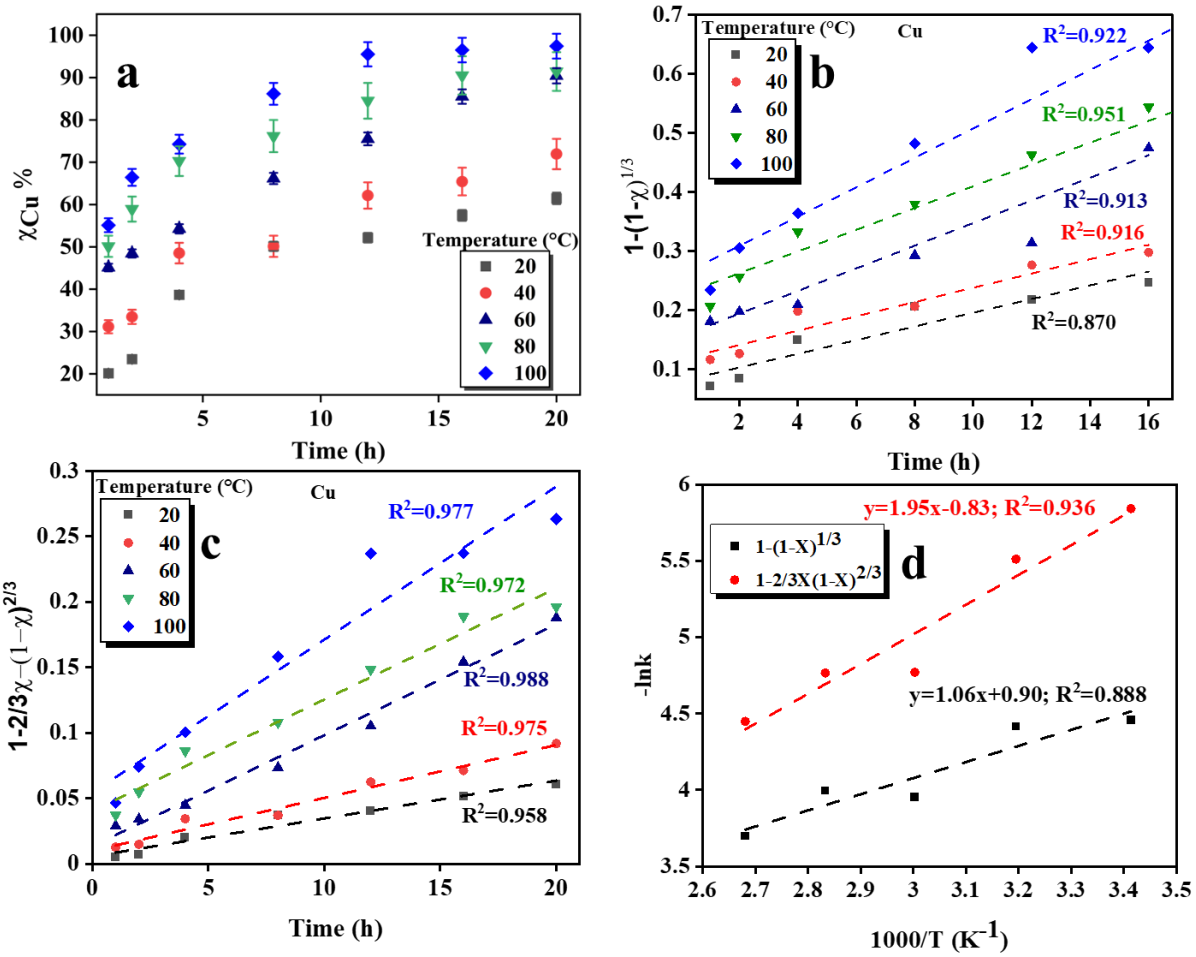

502

503 **Figure 8.** Plots of extraction of Cu with respect to time and temperature (a); $[1-(1-\chi)^{1/3}]$ vs.
504 time at different temperatures and time (b); $[1-2/3\chi-(1-\chi)^{2/3}]$ s time at different temperatures
505 and time (c); Arrhenius plot for extraction of Cu in both models (d).

506 Here, k is the reaction rate constant (h^{-1}), A is the frequency factor, E_a is apparent activation
507 energy (kJ/mol), R is gas constant 8.3145 (J/K-mol), and T is reaction temperature in K. The
508 E_a value of Cu extraction in FA-ChCl comes to 16.21 kJ/ mol in the diffusion-controlled
509 model. It has been thoroughly reported in the literature that E_a less than 25 kJ/mol suggests a
510 diffusion-controlled region, while greater than 30 kJ/mol suggests a chemical reaction-
511 controlled process [54]. The shrinking core model was used by Huang et al. to fit the copper
512 leaching data (in ionic liquids), the reaction was diffusion-controlled and the apparent
513 activation energy calculated was 25.36 kJ/mol [19]. Topcu et al. evaluated activation energy
514 for the dissolution of copper, 8.86 kJ/mol and zinc, 14.48 kJ/mol from copper converter slag

to urea-ChCl DESs [54a]. The activation energy of the dissolution of copper in conventional acids is in the range of 11-55 kJ/mol quite higher than the activation energy of copper extraction in DES [55].

3.6. Mechanism of metal leaching

DESs have an interaction of hydrogen bond donors and acceptors and form hydrogen bonds, hence conferring high dissolution properties. Abbott et al. discussed the chemistry of metal complexes with carboxylic acid-choline chloride DESs [34]. There was a correlation between the solubility of metal oxide in malonic acid-choline chloride and HCl. It was concluded that the proton acts as an oxygen acceptor, forming metal complexes. Detailed analysis of metal complexes revealed the formation of MCl_x^- in most choline chloride DESs [34]. Figure S3 reveals the map of the electrostatic potential calculation of choline chloride, which reveals that chloride ions have the most negative electrostatic potential values at an iso value of 0.02. The electrostatic potential is an important descriptor to understand the reactive behaviour of molecules such as to determine nucleophilic and electrophilic sites in molecules. In choline chloride surface analysis chloride has the most negative potential, hence more prone to electrophilic attack [56]. Hartley et al. investigated the metal solubility in diols-based DESs where metal speciation has proven to be a controlling factor with the dominance of anion of the solvent [57]. Organic acids supply protons and ligands to dissolve metals by acidification and complexation reactions. Organic acid dissociates to protons (H^+) and promotes dissolution. Interactions of metal with organic acids have been discussed in the literature [58]. Nevertheless, there is still a lack of literature and understanding of metal dissolution in organic acid based DESs.

$$RCOOH + H_2O \rightleftharpoons RCOO^- + H_3O^+ \qquad (10)$$

Proton reduction leads to hydrogen and oxidizes metal.

$$2H_3O^+ + 2e^- \rightarrow H_2 + 2H_2O \qquad (11)$$

Complexation reaction occurs alike formate in formic acid and acetate in acetic acid to form stable complex as denoted by equation (12)

$$HCOO^- + M(H_3O^+) \longrightarrow RCOOM + H_2O \qquad (12)$$

Another reason for an increase in metal extraction with the addition of H_2O_2 is the formation of peroxy carboxylic acid; in the case of formic acid, performic acid is formed as shown in *(13)* [59]:

$$HCOOH + H_2O_2 \rightarrow HCOOOH + H_2O \qquad (13)$$

Performic acid has high oxidizing power; hence it oxidizes metal (14).

$$HCOOOH + M + 2H \rightarrow HCOOH + H_2O + M^{2+} \qquad (14)$$

Urea-ChCl DES form metal complex anion [$M_xClO(urea)^-$] from its metallic oxides or sulphate forms. Urea act as a ligand and forms metal complexes anions.

$$Zn^{2+} + HOC_2N(CH_3)3Cl + NH_2CONH_2 \rightarrow \mathrm{ZnOCl(NH_2CONH_2)_2} \qquad (15)$$

The energy difference between the Highest Occupied Molecular Orbitals (HOMO) and the Lowest Unoccupied Molecular Orbital (LUMO) of a complex is a crucial factor that helps in understanding the electron properties and reactivity. High and low energy difference has a significant implication for the complex's behaviour. The energy difference of HOMO LUMO of metal complexes is illustrated in Table S5. Formic acid interaction with copper has the lowest energy gap, which reveals its higher reactivity with the complex as compared to other hydrogen bond donors. However, the low energy gap of oxalic acid interaction with copper reveals its tendency to form copper oxalate. Figure S4 shows the interaction of the Cu4 cluster with different electron-deficient sites of components of DES.

Eh-pH diagram, commonly known as the Pourbaix diagram, aids in understanding the behavior of individual metals in aqueous solutions. Materials project an open-source platform, was utilized to plot Eh-pH diagram of Fe, Cu, Ni, Zn and Sn as shown in Figure S2 (a-e) [60]. Fe^{2+}, Cu^{2+}, Zn^{2+}, Ni^{2+} and Sn^{2+} are the major metal species present in solution.

Standard electrode potential of (metals and H_2O_2) and pH of all DES are tabulated in Tables S2 and S3, respectively. Electrode potential differences of Fe, Cu, Zn, Ni, Sn and H_2O_2 are 1.336 V, 1.436 V, 2.536 V, 2.026 V and 1.63 V, respectively. Considering the Eh-pH diagram of all metals, Fe^{2+}, Cu^{2+}, Zn^{2+}, Ni^{2+} and Sn^{2+} species exist in the acidic pH range above -0.5 V, -0.4 V, -0.8 V, -0.2 V and -0.5 V, respectively. Metal species form metal complexes as denoted by equation (12-13) resulting in metal extraction. For tin extraction in oxalic acid, it was presumed to form tin oxalate. Wang et al. discussed the reduction of Sn (IV) to Sn (II) by E-pH diagram [51]. Sn^{4+} has a stable region in the highly acidic environment; however, the required pH range for the stable region of Sn^{2+} is below pH 3. Compared to sulphuric acid and hydrogen peroxide, E ($CO_2/H_2C_2O_4$) reduction potential is -0.59 V, while E(Sn^{4+}/Sn^{2+}) is 0.15; hence thermodynamically oxalic acid can reduce Sn (IV) to Sn (II), thereby has higher extraction.

3.7. Separation of metals from leached solution

Cementation is an electrochemical phenomenon characterized by the displacement of a metal ion from solution by more reactive metals (sacrificial). Cementation has the advantage of easy operation, cost and high metal recovery and is a common technique used in metallurgy and hydrometallurgy for metal recovery from leached solution. The cementation process is classified as a galvanic process due to its lack of dependence on an external current source. The phenomenon of metal ion reduction in a solution to its metallic form is attributed to the disparity in standard electrode potential between the two metals involved. The equation of the typical cementation process is:

$$aM^{b+} + bN^{0} \rightarrow bN^{a+} + aM^{0} \qquad (16)$$

Here, M^{b+} is the target metal, M^0 is the cemented target metal in metallic form, N^0 is a sacrificial metal used for cementation while N^{a+} is a sacrificial metal used for cementation. Table S3. illustrates the standard electrode potential of metals. The disparity in standard

reduction potentials between copper (Cu) at 0.34 V and zinc (Zn) at -0.76 V instigates the reduction of copper ions into their elemental form. The standard electrode potentials of copper and zinc are illustrated by

$Cu\ (s) \rightarrow Cu^{2+}\ (aq) + 2e^{-}$ -0.34 *(17)*

$Zn^{2+}(aq) + 2e^{-} = Zn\ (s)$ -0.76 *(18)*

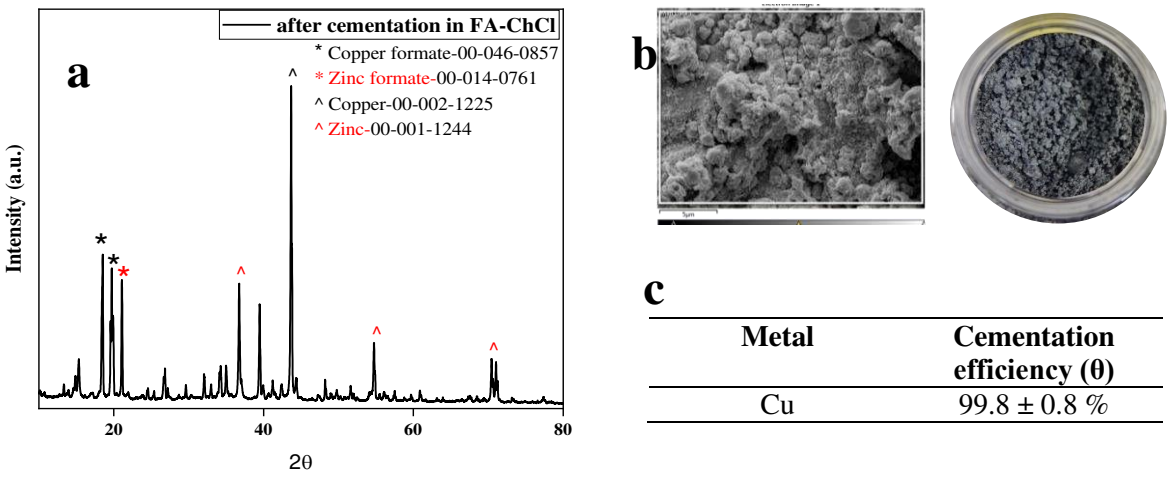

Metal	Cementation efficiency (θ)
Cu	99.8 ± 0.8 %

Figure 9. XRD of recovered powder after cementation from FA-ChCl leached solution (a). FESEM of recovered salt along with visual representation (b). Cementation efficiency of copper from FA-ChCl leached solution using zinc dust (c).

As discussed in our previous paper by Jadhao et al. (2023), the cementation of copper is thermodynamically feasible[52]. An optimized metal leached solution of FA-ChCl was used for this process. At room temperature, metallic zinc powder was added to the leached FA-ChCl solution. The cementation efficiency of copper was observed to be 99.8 ± 0.8 %. However, XRD of recovered powder reveals the presence of copper formate along metallic copper. Figure 9 depicts the XRD of recovered powder after cementation along with FESEM and cementation efficiency.

3.8. Proposed integrated process.

The cumulative multistage leaching process was employed for the selective extraction of metals from PCBs taking 5 g of TPCBs. Initially, 1M Oxalic acid was used to leach Sn from the PCB for 1 h, in 1/20 g/mL ratio at 80 °C, 300 rpm. ICP-MS analysis of leachate revealed

that 93.5 ± 0.4 % of Sn was leached in 1M oxalic acid solution. Alongside, iron extraction was 34.7 ±1.2 % and 10-8 % of Cu in the solution. Further, the solid residue was washed and treated with Urea-ChCl for 16 h, 1/30 g/mL ratio, 80 °C, 400 rpm to extract 90.3 ±1.3 % of zinc. The solid residue was washed and dried and treated with FA-ChCl DES to extract 90 ± 0.9 % Cu, 89 ± 0.2 % Fe, and 88 ± 1.9 % Ni in a leachate solution. Figure 10 depicts the proposed process flowsheet.

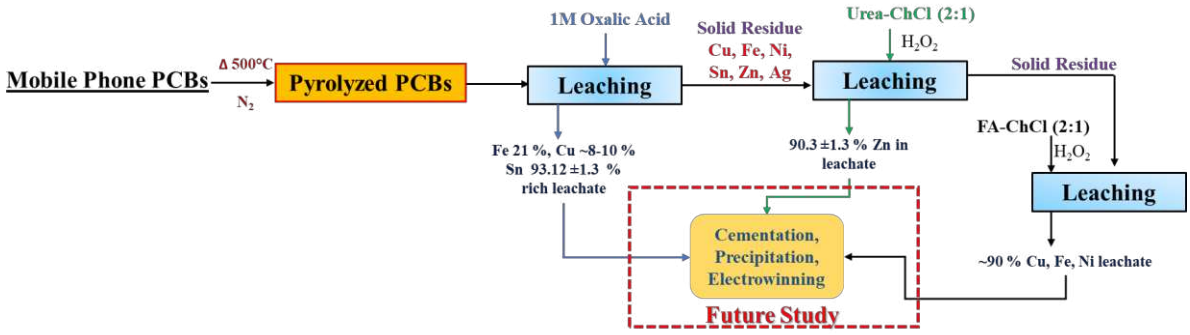

Figure 10. Flowsheet of proposed work for selective extraction of metals from PCBs

There are various aspects in metal extraction from DES which is still not much explored. Exploration of electrowinning integrated with DES metal extraction can be done. The integrated process environmental impact could be evaluated using LCA studies. Alongside, scaleup study to set up greener technology alternative to conventional technology ought to be explored.

4. Conclusion:

In this work, DESs (FA-ChCl, Urea-ChCl) and organic acid have been tested as potential leaching agents for the selective extraction of metals from PCBs. Leaching experiments states that FA-ChCl showed high copper, iron, and nickel solubility in the range of 10^5 ppm while negligible solubility of Zn. However, Urea-ChCl was observed to be selective in the solubility of Zn. Metal leaching experiments in FA-ChCl with H_2O_2 uncover that extraction of Cu, Fe, Ni, and Zn is greater than 90 % at optimized conditions (100 °C, 1/30 g/mL, 16 h, 300 rpm). Zn extraction from TPCBs was observed to be 90.4 ± 2.9 % at (100 °C, 1/20 g/mL,

21 h, 400 rpm). 1M oxalic acid selectively extracted 92.3 ± 2.09 % Sn from TPCBs under optimal conditions (1 h, 80 °C, 1/20 g/mL). The diffusion-controlled reaction is suggested by a shrinking core model-based kinetic investigation of copper extraction in FA-ChCl. The apparent activation energy of copper was 16.21 kJ/ mol. Metal extraction mechanism in DES is a two-step process with a major complexation reaction of metals with ligands of hydrogen bond donor or acceptor anion, which is explained by Eh-pH diagram of metals. This study provided a detailed investigation of metal extraction in green solvents, which paved a new approach for the selective extraction of metals from PCBs. Further analysis of the mechanism of metal extraction in the green solvent must be studied in detail, correlating theoretical calculations with experimental results to further understand at a molecular scale. Moreover, detailed research on metal speciation in DES systems is required to fully comprehend the mechanism.

AUTHOR INFORMATION

Corresponding Author

Kamal Kishore Pant - Green and Sustainable Engineering Laboratory, Department of Chemical Engineering, Indian Institute of Technology Delhi, New Delhi, 110016, India.

Department of Chemical Engineering, IIT Roorkee, Roorkee, 247667, India

Email: kkpant@chemical.iitd.ac.in , dr.kkpant@gmail.com

David Harbottle- School of Chemical and Process Engineering, University of Leeds, Leeds, LS29JT, United Kingdom. Email: D.Harbottle@leeds.ac.uk

Other Authors

Snigdha Mishra- Green and Sustainable Engineering Laboratory, Department of Chemical Engineering, Indian Institute of Technology Delhi, New Delhi, 110016, India.

School of Chemical and Process Engineering, University of Leeds, Leeds, LS29JT, United Kingdom

Timothy. N. Hunter- School of Chemical and Process Engineering, University of Leeds, Leeds, LS29JT, United Kingdom

AUTHOR CONTRIBUTIONS

The manuscript was written through contributions of all authors. All authors have given approval to the final version of the manuscript.

ACKNOWLEDGMENT

This paper is partly based on a Commonwealth Trust split-site Ph.D. studentship awarded to Snigdha Mishra. No grant reference number is available for this award to Snigdha Mishra. The authors would like to thank the Office of the Principal Scientific Adviser to the Government of India for providing a research grant under DRIIV. The DFT work was undertaken on ARC3, part of the High-Performance Computing facilities at the University of Leeds, UK.

ABBREVIATIONS

B3LYP: Beck's three parameter functional Lee Yang Parr

ChCl: Choline Chloride

DESs: Deep Eutectic Solvents

DFT: Density Functional Theory

EG: Ethylene Glycol

EG-ChCl: Ethylene Glycol-Choline chloride

FA: Formic Acid

FA-ChCl: Formic Acid-Choline chloride

FTIR: Fourier Transform Infrared Spectroscopy

HBA: Hydrogen Bond Acceptor

HBD: Hydrogen Bond Donor

ILs: Ionic Liquids

MA-ChCl: Malonic Acid-Choline chloride

OA: Oxalic Acid

OA-ChCl: Oxalic Acid-Choline chloride

PCB: Printed Circuit board

TPCBs: Thermally treated printed circuit boards

TGA: Thermo Gravimetric Analysis

Urea-ChCl: Urea-Choline chloride

References

[1] G. Chauhan, P. J. Kaur, K. K. Pant, K. D. P. Nigam, Sustainable Metal Extraction from Waste Streams *Wiley*, **2020**.

[2] V. B. Forti, C. P. Kuehr, G. Ruediger Bel, United Nations University (UNU)/United Nations Institute for Training and Research (UNITAR), International Telecommunication Union (ITU) & International Solid Waste Association (ISWA), Bonn/Geneva/Rotterdam, **2020**, p. 120.

[3] J. Szałatkiewicz, *Pol. J. Environ. Stud.* **2014**, *23*, 2365-2369.

[4] R. Nithya, C. Sivasankari, A. Thirunavukkarasu, *Environmental Chemistry Letters* **2020**, 1347-1368.

[5] aJ. Sohaili, S. K. Muniyandi, S. S. Mohamad, *International Journal of Scientific & Engineering Research* **2012**, *3*, 12-18; bM. X. Ni, Hanxi Chi, Yong Yan, Jianhua Buekens, Alfons Jin, Yuqi Lu, Shengyong, *Waste Management* **2012**, *32*, 568-574.

[6] Z. Sun, Y. Xiao, H. Agterhuis, J. Sietsma, Y. Yang, *Journal of Cleaner Production* **2016**, *112*, 2977-2987.

[7] M. Xue, G. Yan, J. Li, Z. Xu, *Environ. Sci. Technol.* **2012**, *46*, 10556-10563.

[8] M. Kaya, *Waste Management* **2016**, *57*, 64-90.

[9] G. Zhang, Y. He, H. Wang, T. Zhang, S. Wang, X. Yang, W. Xia, *Waste Management* **2017**, *64*, 228-235.

[10] C. B. Tabelin, I. Park, T. Phengsaart, S. Jeon, M. Villacorte-Tabelin, D. Alonzo, K. Yoo, M. Ito, N. Hiroyoshi, *Resources, Conservation and Recycling* **2021**, *170*.

[11] P. Stuhlpfarrer, S. Luidold, H. Antrekowitsch, *J. Hazard. Mater.* **2016**, *307*, 17-25.

[12] A. E. Akcil, Ceren; Gahan, Chandra Sekhar; Ozgun, Mehmet; Sahin, Merve; Tuncuk, Aysenur, *Waste Management* **2014**, *45*, 258-271.

[13] A. Tripathi, M. Kumar, S. D.C., A. Agrawal, S. Chakravarty, T. R. Mankhand, *International Journal of Metallurgical Engineering* **2012**, *1*, 17-21.

[14] P. K. Choubey, R. Panda, M. K. Jha, J. C. Lee, D. D. Pathak, *Separation and Purification Technology* **2015**, *156*, 269-275.

[15] M. S. A. Lee, J. G. Ahn, J. W., *Hydrometallurgy* **2003**, *70*, 23-29.

[16] G. Chauhan, P. R. Jadhao, K. K. Pant, K. D. P. Nigam, *Journal of environmental chemical engineering* **2018**, *6*, 1288-1304.

[17] aA. Golzary, M. A. Abdoli, *Journal of CO_2 Utilization* **2020**, *41*, 101265; bC. H. C. M.-R. Janssen, Norma A. Aguilar-Martínez, Martha Kobrak, Mark N., *International Reviews in Physical Chemistry* **2015**, *34*, 591-622; cA. P. F. Abbott, Gero; Hartley, Jennifer; Ryder, Karl S., *Green Chemistry* **2011**, *13*, 471-481; dG. R. T. Jenkin, A. Z. M. Al-Bassam, R. C. Harris, A. P. Abbott, D. J. Smith, D. A. Holwell, R. J. Chapman, C. J. Stanley, *Minerals Engineering* **2016**, *87*, 18-24.

[18] F. Xiu, Rong, Y. Qi, F. Zhang, Shen *Waste Management* **2015**, *41*, 134-141.

[19] J. Huang, M. Chen, H. Chen, S. Chen, Q. Sun, *Waste Management* **2014**, *34*, 483-488.

[20] Y. Barrueto, P. Hernández, Y. Jiménez, J. Morales, *J. Mater. Cycles Waste Manag.* **2021**, *23*, 2028-2036.

[21] E. L. Smith, , A. P. Abbott, , K. S. Ryder, , **2014**, *114*, 11060-11082.

[22] B. B. Hansen, S. Spittle, B. Chen, D. Poe, Y. Zhang, M. Klein, A. Horton, L. Adhikari, T. Zelovich, B. W. Doherty, B. Gurkan, E. J. Maginn, A. Ragauskas, M. Dadmun, T. A. Zawodzinski, G. A. Baker, M. E. Tuckerman, R. F. Savinell, J. R. Sangoro, *Chemical Reviews* **2021**, *121*, 1232-1285.

[23] R. Marin Rivera, G. Zante, J. M. Hartley, K. S. Ryder, A. P. Abbott, *Green Chemistry* **2022**, *24*, 3023-3034.

[24] A. P. B. Abbott, David; Capper, Glen ;Davies, David; L.; Rasheed, Raymond K., *Journal of American Chemical Society* **2004**, *126*, 9142-9147.

[25] aE. L. Smith, A. P. Abbott, K. S. Ryder, *Chemical Reviews* **2014**, *114*, 11060-11082; bI. V. Zinov'eva, A. Y. Fedorov, N. A. Milevskii, Y. A. Zakhodyaeva, A. A. Voshkin, *Theoretical Foundations of Chemical Engineering* **2021**, *55*, 663-670; cP. Cen, K. Spahiu, M. Tyumentsev, S. Foreman, M. R. S. J., *Physical Chemistry Chemical Physics* **2020**, *22*, 11012-11024.
[26] S. Riaño, M. Petranikova, B. Onghena, T. Vander Hoogerstraete, D. Banerjee, M. R. S. Foreman, C. Ekberg, K. Binnemans, *RSC Advances* **2017**, *7*, 32100-32113.
[27] S. B. Anggara, Francesca; Harris, Robert C.; Hartley, Jennifer M.; Frisch, Gero; Jenkin, Gawen R.T.; Abbott, Andrew P., *Green Chemistry* **2019**, *21*, 6502-6512.
[28] A. Entezari-Zarandi, F. Larachi, *Journal of Rare Earths* **2019**, *37*, 528-533.
[29] A. Bakkar, *J. Hazard. Mater.* **2014**, *280*, 191-199.
[30] aT. Hanada, M. Goto, *ACS Sustainable Chemistry & Engineering* **2021**, *9*, 2152-2160; bF. Pena-Pereira, J. Namieśnik, *ChemSusChem* **2014**, *7*, 1784-1800; cB. Li, Q. Li, Q. Wang, X. Yan, M. Shi, C. Wu, *Physical Chemistry Chemical Physics* **2022**, *24*, 19029-19051; dP. G. Schiavi, P. Altimari, E. Sturabotti, A. Giacomo Marrani, G. Simonetti, F. Pagnanelli, *ChemSusChem* **2022**, *15*, e202200966; eM. K. Tran, M. T. F. Rodrigues, K. Kato, G. Babu, P. M. Ajayan, *Nature Energy* **2019**, *4*, 339-345.
[31] S. Wang, Z. Zhang, Z. Lu, Z. Xu, *Green Chemistry* **2020**, *22*, 4473-4482.
[32] A. Łukomska, A. Wiśniewska, Z. Dąbrowski, J. Lach, K. Wróbel, D. Kolasa, U. Domańska, *Molecules* **2022**, *27*, 4984.
[33] M.-L. Doche, A. Mandroyan, M. Mourad-Mahmoud, V. Moutarlier, J.-Y. Hihn, *Chemical Engineering and Processing: Process Intensification* **2017**, *121*, 90-96.
[34] A. P. C. Abbott, Glen; Davies, David L.; McKenzie, Katy J.; Obi, Stephen U., *Journal of Chemical & Engineering Data* **2006**, *51*, 1280-1282.
[35] I. de Marco, B. M. Caballero, M. J. Chomón, M. F. Laresgoiti, A. Torres, G. Fernández, S. Arnaiz, *Journal of Analytical and Applied Pyrolysis* **2008**, *82*, 179-183.
[36] Y. Z. Li, Nengwu Wei, Xiaorong Cui, Jiaying Wu, Pingxiao Li, Ping Wu, Jinhua Lin, Yimin, *Process Safety and Environmental Protection* **2020**, *133*, 137-148.
[37] A. D. Becke, *The Journal of Chemical Physics* **1993**, *98*, 5648.
[38] aR. Panda, P. R. Jadhao, K. K. Pant, S. N. Naik, T. Bhaskar, *J. Hazard. Mater.* **2020**, *395*, 122642; bP. R. Jadhao, E. Ahmad, K. K. Pant, K. D. P. Nigam, *Waste Management* **2020**, *118*, 150-160.
[39] M. Gudorf, Z. Lazarova, K. Schügerl, *Hydrometallurgy* **1996**, *42*, 125-130.
[40] aC. Werner, C. Steinberg, J. Maurer, H. Zumaque*, Vol. US 8,277,774 B2*, GOIG 9/00 (2006.01) ed. (Ed.: U. S. Patent), Honeywell International, Morristown, NJ (US), United States, **2012**; bY. L. Wang, Bingbing Sun, Hu Huang, Yanfang Han, Guihong, *Journal of Cleaner Production* **2022**, *342*, 130955.
[41] S. Mishra, A. Pandey, K. K. Pant, B. Mishra, *Journal of Molecular Liquids* **2023**, *383*, 122142.
[42] A. R. Harifi-Mood, R. Buchner, *Journal of Molecular Liquids* **2017**, *225*, 689-695.
[43] P. R. Jadhao, A. Pandey, K. K. Pant, K. D. P. Nigam, *Journal of environmental management* **2021**, *296*, 113154.
[44] R. Gautam, N. Kumar, J. G. Lynam, *Journal of Molecular Structure* **2020**, *1222*, 128849.
[45] X. B. Li, Koen, *Chemical Reviews* **2021**, *121*, 4506-4530.
[46] J. W. Z. Moffett, Rod G., *Environ. Sci. Technol.* **1987**, *21*, 804-810.
[47] D. W. Colcleugh, W. F. Graydon, *Canadian Journal of Chemistry* **1962**, *40*, 1497-1509.
[48] aC. Silva, G. Zeba, C. Rocha, P. Gismonti, J. Afonso, R. Silva, C. Vianna, J. Mantovano, *Quimica Nova* **2020**, *43*, 914-922; bU. Jadhav, Su, C., Hocheng, H., *RSC Advances* **2016**, *6*, 43442-43452.

[49] P. R. Jadhao, G. Chauhan, K. K. Pant, K. D. P. Nigam, *Waste Management* **2016**, *57*, 102-112.
[50] A. Saini, A. Kumar, P. S. Panesar, A. Thakur, *Applied Food Research* **2022**, *2*, 100211.
[51] Y. Wang, B. Liu, H. Sun, Y. Huang, G. Han, *Journal of Cleaner Production* **2022**, *342*, 130955.
[52] P. R. Jadhao, S. Mishra, A. Singh, K. K. Pant, K. D. P. Nigam, *Journal of Environmental Management* **2023**, *335*, 117581.
[53] K. C. Liddell, *Hydrometallurgy* **2005**, *79*, 62-68.
[54] aM. A. Topçu, A. Rüşen, Ö. Küçük, *Waste Management* **2021**, *132*, 64-73; bY. Han, X. Yi, R. Wang, J. Huang, M. Chen, Z. Sun, S. S. Sun, Jiancheng, *Separation and Purification Technology* **2020**, *253*, 117463.
[55] M. D. Turan, Z. A. Sari, A. Demiraslan, *Metallurgical and Materials Transactions B* **2019**, *50*, 1949-1956.
[56] F. De Proft, J. M. L. Martin, P. Geerlings, *Chemical Physics Letters* **1996**, *256*, 400-408.
[57] J. M. Hartley, C.-M. Ip, G. C. H. Forrest, K. Singh, S. J. Gurman, K. S. Ryder, A. P. Abbott, G. Frisch, *Inorganic Chemistry* **2014**, *53*, 6280-6288.
[58] aS. A. Wasay, S. Barrington, S. Tokunaga, *Water, Air, and Soil Pollution* **2001**, *127*, 301-314; bG. P. Nayaka, K. V. Pai, J. Manjanna, S. J. Keny, *Waste Management* **2016**, *51*, 234-238.
[59] H.-P. Y. Li, Chris M. Brinkmeyer, Robin Zhang, Saijin Ho, Yi-Fang Xu, Chen Jones, Whitney L. Schwehr, Kathleen A. Otosaka, Shigeyoshi Roberts, Kimberly A. Kaplan, Daniel I. Santschi, Peter H., *Environ. Sci. Technol.* **2012**, *46*, 4837-4844.
[60] A. Jain, Ong, Shyue Ping, Hautier, Geoffroy Wei Chen, William Davidson Richards, Stephen Dacek, Shreyas Cholia, Dan Gunter, David Skinner,Gerbrand Ceder, and Kristin A. Persson, *APL Materials* **2013**, *1*, 011002.